Modelling evolution of anisotropy in fabric and texture of polar ice

Sérgio H. FARIA, Dimitri KTITAREV, Kolumban HUTTER

Institute of Mechanics, Darmstadt University of Technology, Hochschulstrasse 1, D-64289 Darmstadt, Germany
E-mail: faria@mechanik.tu-darmstadt.de

ABSTRACT. We present a simulation tool, based on a cellular automaton algorithm developed by D. Ktitarev and others, for the modelling of fabric and texture evolution in polycrystalline ice. The numerical results for the case of vertical uniaxial compression are compared with data obtained from boreholes GRIP–GISP2 in Greenland. A reasonable agreement is obtained, and guidelines are presented for further formulation of more realistic simulations. In particular, we discuss the rise of girdle-type fabrics, as well as the importance of intra- and intercrystalline stresses, temperature and impurity effects on the evolving ice microstructure.

INTRODUCTION

In most aspects, monocrystalline ice is a very anisotropic material. As discussed more than a century ago by Nordenskjöld (1861), some of its basic features can be well represented by considering a right hexagonal monocrystalline prism (see Fig. 1). Basal planes (0001) are the planes of densest packing of molecules and lie orthogonal to the c axis, which is the axis of optical and crystallographic (hexagonal) symmetry of the crystal. The prismatic faces $\{1\bar{1}00\}$, on the other hand, are parallel to this axis, while pyramidal planes, like $\{1\bar{1}01\}$, are those which cross the bulk of the prism.

In the range of plastic deformation, the anisotropy of ice is quite marked, being expressed through the fact that ice single crystals creep very readily by basal slide. This kind of deformation, also called *easy glide* creep, has been recognized in ice since the end of the 19th century (McConnel, 1891; see also Faria and Hutter, 2001), and was later confirmed in a number of different mechanical tests and field observations (see, e.g., the reviews of Steinemann, 1958; Glen, 1975; Weertman, 1983). Such a highly anisotropic plasticity renders the mechanics of the polycrystalline ice of glaciers and ice sheets a rather complex matter. Numerous attempts have been made to establish a "universal" flow law, relating the strain rate to the stress, which could be used in simulations of ice dynamics. This sought-after flow law has proven to be strongly dependent, among other factors, on the anisotropic distribution of crystallographic orientations (*fabric*) slowly induced by ice flow (Budd and Jacka, 1989; Paterson, 1991; Alley, 1992). Additionally, recent studies (Hutter and Vulliet, 1985; Thorsteinsson and others, 1999; Cuffey and others, 2000) have suggested that the distribution of grain-sizes (*texture*) and/or impurity content may play some role.

Usually, anisotropic ice models reckon the crystalline deformation is produced entirely by basal glide, under the assumption that the stress is uniform, i.e. it is the same for all grains of the polycrystal (Sachs, 1928; Reuss, 1929). In this case, it is expected that additional mechanisms (often not considered in the modelling), such as diffusional flow, dislocation climb, kink bands, grain-boundary sliding and migration, polygonization and dynamic recrystallization, can fulfil the necessity of coherence within the aggregate. Although many models based on these two premises (easy glide creep and uniform stress) were proposed to simulate the dynamics of ice fabrics, they usually considered only the *kinematic rotation* of c axes due to the applied stress (e.g. Azuma and Higashi, 1985; Fujita and others, 1987; Alley, 1988; Lipenkov and others, 1989; Lliboutry, 1993; Van der Veen and Whillans, 1994; Gagliardini and Meyssonnier, 1999; Thorsteinsson and others, 1999). Clearly, consideration of c-axis rotation alone builds an incomplete picture of the evolving anisotropy, since microscopic processes referred to by the common term *recrystallization*, such as *grain growth*, bending and fragmentation of existing crystals (*polygonization*) as well as the nucleation of entirely new crystals (*dynamic recrystallization*), can strikingly affect the final grain-sizes and c-axis fabric.

Whereas recrystallization has been intensively investigated and modelled in metallurgy (e.g. Derby, 1991; Humphreys and Hatherly, 1996; Doherty and others, 1997), in glaciological models it has often been neglected, despite recognition of its importance for the mechanics of polycrystalline ice (Paterson, 1991; Duval and Castelnau, 1995; Gow and others, 1997; De La Chapelle and others, 1998; Jacka
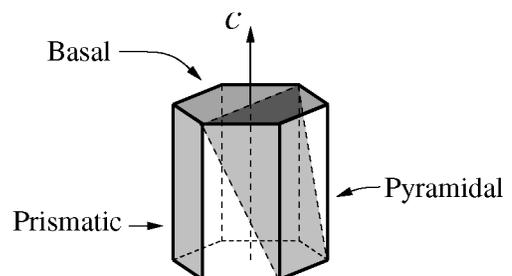
Fig. 1. Sketch of a single ice crystal in the form of a right hexagonal prism. Three types of crystallographic planes are indicated.

545

and Li, 2000). Moreover, pioneering approaches to incorporate dynamic recrystallization in ice models (e.g. Van der Veen and Whillans, 1994) are usually impaired by their artificial mechanisms based on physically flimsy grounds.

The present work represents a preliminary attempt to construct a simulation tool, grounded on existing knowledge of ice microstructure evolution, which could be applied to test different physical hypotheses assumed in anisotropic ice models. The model is based on a Cellular Automaton (CA) algorithm developed by D. Ktitarev, in collaboration with G. Gödert and K. Hutter (personal communication from D. Ktitarev, 2001), and contains several coupled microstructural mechanisms which promote changes in fabric and texture, such as grain growth, polygonization and dynamic recrystallization. At the present stage, however, the influence of impurity concentrations is not considered, due to lack of information for its mathematical modelling.

It has been shown in recent publications in the material science literature that the CA method represents a useful tool which is sufficiently flexible to model recrystallization processes (Hesselbarth and Göbel, 1991; Goetz and Seetharaman, 1998a, b; Marx and others, 1999). Like the finite-element method, which has also recently been employed to simulate the micromechanics of ice (Meyssonnier and Philip, 2000), CA requires a partition of the body into discrete areas, so-called cells, which are associated with generalized state variables and arranged in a regular environment (e.g. a lattice structure). CA models are generally characterized by their local transformation rules and are more flexible than finite-element methods with respect to the interaction of cells, modelling singularities and spontaneous effects.

THE MODEL

Theoretical grounds

The main objective of the model is to reproduce the typical features of texture and fabric of ice polycrystals as they evolve by descending from the top into deeper layers of an ice sheet. Aiming for a definite problem, the present simulation focuses on the evolution of a small sample of ice, formed from snow on a free surface located in the dome of a hypothetical ice sheet. As the mass of ice flows down to the bottom, it deforms under the action of vertical compression by the layers above it. For simplicity, we consider at this stage only the ideal situation where the compression is constant and no additional shear stresses occur (i.e. unconfined compression). The sample is assumed to be extremely thin, like a shallow pillbox or a slender slice of an ice core (Fig. 2, top). This yields the description of the polycrystalline piece to a two-dimensional aggregate, and allows the assumption that the sample has the same type of microstructure and experiences the same mechanical processes as the surrounding material. Moreover, for the simple case of uniaxial compression considered here, it is expected that the kinematic rotation as well as the recrystallization processes possess rotational symmetry. From these considerations it follows that the problem of characterizing the polycrystalline microstructure is reduced to a one-dimensional description of the aggregate (Fig. 2, centre) by two structural quantities, namely, the distribution of grain-sizes and the crystallographic orientations. Since the proposed algorithm aims at a qualitative description, only dimensionless variables and parameters will be considered.

To discretize the problem according to the CA method,
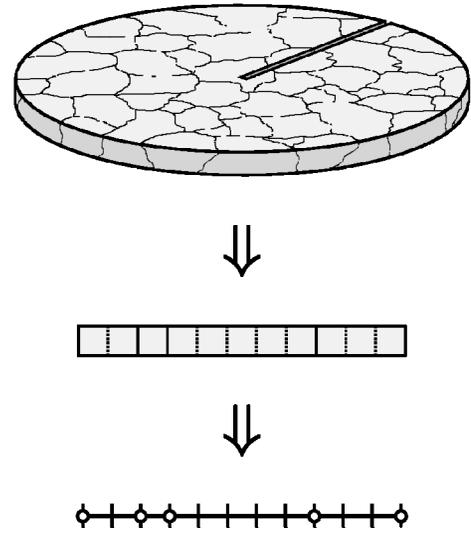
Fig. 2. Top: model of ice sample employed in the CA simulation. The diameter is approximately that of an ice core ($\approx 10\,cm$), while the thickness is assumed to be many orders of magnitude smaller than this. Centre: radial slice of the sample. Cell divisions (dashed lines) and grain boundaries (solid lines) are presented. Bottom: one-dimensional representation of the sample used in the algorithm. Cell divisions (bars) and grain boundaries (circles) are indicated.

we take a one-dimensional lattice of N equal cells (Fig 2, bottom). Collections of neighbouring cells with the same crystallographic orientation represent the M grains of the polycrystal, in such a way that each grain $k\,(k = 1, \ldots, M)$ contains l_k cells. Every cell $i\,(i = 1, \ldots, N)$ corresponds to a grain of minimum size $D_{\min}$ (typically of the order of a millimetre), and therefore the size of a grain k is computed by $D_k = D_{\min} l_k$. Of course, M and l_k can vary in time, while N and $D_{\min}$ are constant. The basic dynamical quantity of the algorithm is the dislocation density of the cells ρ_i, which describes the length of dislocations per unit volume. Dislocations are created in ice during its deformation. Their production depends on the orientation of the particular grain, which is defined by the angle θ_k between the c-axis unit vector $\boldsymbol{n}_k$ and the vertical. Texture and fabric changes in deforming ice develop as a result of kinematic (strain-induced) rotation and recrystallization processes, i.e. grain growth, polygonization and dynamic recrystallization, this last taking place when a critical value of the dislocation density is reached.

Kinematic rotation, normal grain growth and polygonization

Strain-induced rotation of grains is governed by a kinematic equation, which is easily derived using standard arguments of the micromechanical theory of crystals (see, e.g., Asaro, 1983). For the case of ice under uniaxial compression, it can be shown (Svendsen and Hutter, 1996; Gödert and Hutter, 1998, 2000) that this equation reads

$$\frac{\mathrm{d}\boldsymbol{n}_k}{\mathrm{d}t} = -\boldsymbol{W}_k^{\mathrm{I}}\boldsymbol{n}_k, \text{ with } \boldsymbol{W}_k^{\mathrm{I}} = \frac{\dot{\gamma}_k}{2}(\boldsymbol{s}_k \otimes \boldsymbol{n}_k - \boldsymbol{n}_k \otimes \boldsymbol{s}_k),$$
(1)

where $\boldsymbol{W}_k^{\mathrm{I}}$ is the inelastic (or plastic) spin tensor, $\dot{\gamma}_k$ is the basal shearing rate and $\boldsymbol{s}_k$ is a unit vector orthogonal to $\boldsymbol{n}_k$ and parallel to the shear direction — all these quantities related to a given grain k — while $\otimes$ denotes the tensor

product. Considering the slow changes in the stress state and the comparatively low deviatoric stresses expected to occur near to the dome of an ice sheet (e.g. below 50 kPa in Greenland's Summit, according to Greve and others, 1999), it becomes physically reasonable to propose, in a first approximation, a linearly viscous relation for the basal shearing rate $\dot{\gamma}_k$. This choice, which is not without precedents in the literature (see, e.g., Lile, 1978; Hutter 1983; Lliboutry, 1993; Meyssonnier and Philip, 1996; Gagliardini and Meyssonnier, 1999), implies that

$$\dot{\gamma}_k = \eta^{-1}\tau_k, \qquad \text{with} \qquad \tau_k = \sigma \sin\theta_k \cos\theta_k, \qquad (2)$$

where τ_k is the resolved shear stress on the basal plane of the crystal k, σ is the compressive stress (assumed the same for all grains of the sample) and the material constant η^{-1} is the basal fluidity (viscosity^{-1}) of the ice crystals. Hence, by recalling the assumed rotational symmetry of the microstructure with respect to the vertical axis of compression, one can deduce from Equations (1) and (2) the evolution equation for θ_k:

$$\frac{d\theta_k}{dt} = -\frac{1}{2}\eta^{-1}\sigma \sin\theta_k \cos\theta_k. \qquad (3)$$

The homogeneous increase of grain-size, driven by the surface energy of grain boundaries, is called *normal grain growth*. According to Gow (1969) (see also Paterson, 1994; De La Chapelle and others, 1998), for the particular case of polar ice there holds the usual Burke–Turnbull parabolic growth law for the average grain-size

$$D^2(t) = D_0^2 + Kt, \qquad \text{with} \qquad D = \frac{N}{M}D_{\min}, \qquad (4)$$

where the constants D_0 and K denote the initial average grain-size and the normal grain-growth rate, respectively. In the numerical algorithm, the discretization of Equation (4) implies that a fraction $\Phi_{ng} = 1 - D/(D^2 + K)^{1/2}$ of grains are consumed by their larger neighbours at each time-step.

Nevertheless, ice crystals do not grow indefinitely, since they tend to bend and fragment under increasing strain by *polygonization*. Such a crystal breaking can be easily modelled by assuming that, for the case of polar ice, the dislocation density ρ_i is dominated by the density of geometrically necessary dislocations, which are arranged in a dynamic structure of subgrain walls, while the density of statistically stored dislocations is considered negligible (Ashby, 1970; Sandström and Lagneborg, 1975). Hence, we can introduce the misorientation subgrain angle by the formula (cf. Humphreys and Hatherly, 1996; Montagnat and Duval, 2000)

$$\phi_i = \beta\rho_i bD, \qquad \beta \approx 1/2, \qquad (5)$$

where b is the length of the Burgers vector and β is a scaling factor. When the misorientation angle of the cell i exceeds a certain threshold value ϕ_c, then the respective grain k polygonizes at that cell, i.e. it splits into two grains k_1 and k_2 with orientations $\theta_{k_1} = \theta_k - \Delta\theta$ and $\theta_{k_2} = \theta_k + \Delta\theta$ ($\Delta\theta$ of the order of few degrees). Analogously to the normal grain growth, in the numerical algorithm we allow a fraction Φ_{pg} of grains to polygonize, when the corresponding condition above is fulfilled. At this moment it should be clear that such a random update is usually employed in CA simulations of polycrystals when the dynamic rule for the particular grain depends also on its neighbours (see, e.g., Hesselbarth and Göbel, 1991; Goetz and Seetharaman, 1998a, b). In the present simulation, reasonable results have been obtained for $\Phi_{pg} = 20\%$.

Recovery and dynamic recrystallization

Following Montagnat and Duval (2000), we assume that the dislocation density of each cell is balanced by three distinct processes, namely, production by *work-hardening*, reduction by *grain-growth recovery* and decrease by *polygonization recovery*, which are respectively given by

$$\frac{d\rho_i}{dt} = \frac{\dot{\gamma}_k}{bD} - \frac{\alpha\rho_i K}{D^2} - R_{pg}, \qquad \alpha \approx 1, \qquad (6)$$

with α denoting the recovery rate factor, while

$$R_{pg} = \begin{cases} 0, & \text{if } \phi_i < \phi_c, \\ \dfrac{\phi_c K}{2\beta bD^3}, & \text{if } \phi_i \geq \phi_c. \end{cases} \qquad (7)$$

Considering the argumentation of Montagnat and Duval (2000) and results of the measurements of Hondoh and others (1990), other mechanisms of recovery (e.g. by dislocation climb) are not considered in the model.

During *dynamic recrystallization*, new grains, with crystallographic orientations usually differing from those of the surrounding crystals, nucleate and grow rapidly, consuming older grains. In ice sheets, observations in situ show that dynamic recrystallization becomes significant only in the last few hundred metres above the bedrock, where the ice temperature becomes sufficiently high (close to $-10°$C, as argued by Duval and Castelnau, 1995), provided that a sufficient amount of mechanical energy is stored in the grains. Since the influence of temperature is not yet accounted in the modelling, dynamic recrystallization is activated in the simulation only from a certain time-step on, which means that the corresponding modelled ice sample is located below a critical depth.

Currently, there are many hypotheses on the mechanisms of dynamic recrystallization, most of them based on the evidence that nucleation of a new crystal probably occurs at the boundary of an existing grain (Sandström and Lagneborg, 1975; Derby, 1991; Humphreys and Hatherly, 1996; Doherty and others, 1997). Hence, as in the case of polygonization discussed above (see also Hesselbarth and Göbel, 1991; Goetz and Seetharaman, 1998a, b), the program checks a fraction Φ_{rx} of the total number of grains in the system at each time-step, verifying if the dislocation density at their boundary cells exceeds the threshold value $\rho_{rx} = C_{rx}\dot{\rho}^{2m}$, where $\dot{\rho}$ is the average dislocation rate, $m = 0.2$ is the strain-rate sensitivity and C_{rx} is a scaling factor (Peczak and Luton, 1994; Goetz and Seetharaman, 1998a). If the condition is fulfilled, then the boundary cell i is converted into a new grain $i \rightarrow k$ and begins to grow. In the present simulation, we opted for the typical fraction $\Phi_{rx} = 1\%$.

As remarked by Duval and Castelnau (1995) and De La Chapelle and others (1998), dynamic recrystallization is characterized by a very rapid grain-boundary migration rate, i.e. its rate is much higher than that of normal grain growth. To express such an *abnormal grain growth* in the algorithm, at every time-step we let the newly born grain consume up to 10 cells from both right and left. This consumption is possible if the neighbouring grains are not growing abnormally at the same time. The grain ceases to grow if it is hindered by another abnormally growing grain or if the critical size of the steady state $D_{ss} = C_{ss}\dot{\rho}^{-\frac{3}{2}m}$ is reached, with C_{ss} denoting a proportionality factor (Derby, 1991; Goetz and Seetharaman, 1998a, b). The crystallographic orientation of the new grain is prescribed by the hypothesis proposed by Kamb (1972) that the recrystallized
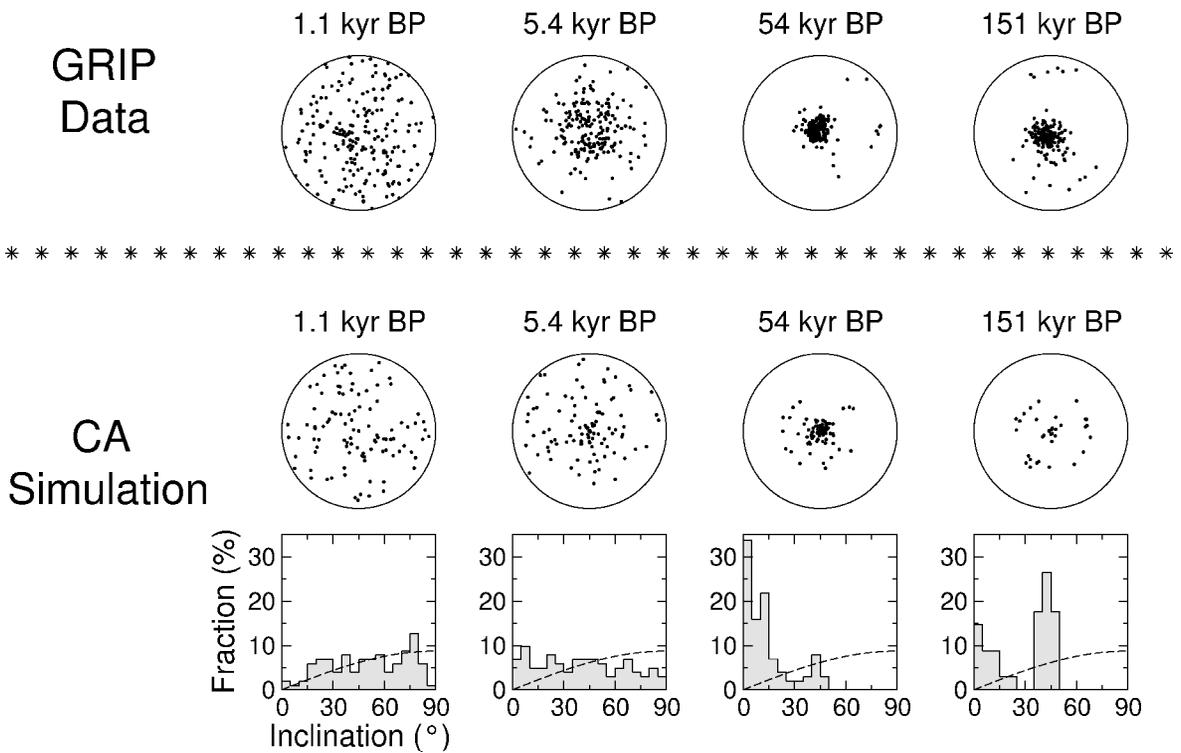
Fig. 3. Comparison of fabric diagrams from GRIP and CA simulation. Correspondent histograms from simulation are also shown, indicating the fraction of c axes at each inclination from the vertical. The sinusoidal curve in histograms (dashed line) corresponds to an isotropic distribution of c axes.

grain takes the orientation of a soft crystal most favourable for plastic deformation by easy glide. In the particular case of vertical compression considered here, this corresponds to an angle $\theta_k = \pi/4$.

Thus, these five rules, namely, increase of dislocation density, kinematic rotation, normal grain growth, polygonization and dynamic recrystallization, are used in the system of grains at each time-step. The first two rules are applied to all grains (sequential update), and the last three are applied to fractions of randomly chosen grains, for the reasons already explained.

COMPARISON WITH DATA FROM ICE CORES AT THE SUMMIT

In this section we compare the results of the CA simulation, as described above, with the microstructural features observed in ice cores from Greenland's Summit, namely, the Greenland Ice Core Project (GRIP) and Greenland Ice Sheet Project 2 (GISP2) ice cores. Of course, there is no pretension to reproduce accurately field observations, since the actual model is still constrained by suitable simplifications to the idealistic situation sketched in the previous section. Nevertheless, this comparison will prove fruitful in determining guidelines for further improvements of the model towards more realistic simulations of polar ice microstructures. The ice-core data utilized in this section were provided by the U.S. National Snow and Ice Data Center, University of Colorado at Boulder, and the World Data Center-A for Paleoclimatology, National Geophysical Data Center, Boulder, CO (see also Thorsteinsson, 1996; Gow and others, 1997; Thorsteinsson and others, 1997) and include fabric, texture, age and impurity data.

For the CA simulation we choose a one-dimensional

grid of $N = 1000$ cells. At the initial configuration, the same dislocation density is attributed to each cell, and different grain-sizes are uniformly distributed over $M_0 = 100$ grains, so that the initial mean grain-size is equal to 10 cells. The program executes 10 000 discrete time-steps of 25 years, corresponding to 250 000 years BP. In order to avoid the complications of the initial regime of deformation, where primary creep, firn densification and other transient processes dominate, the simulation starts 500 years BP, which corresponds to a depth of about 145 m for GRIP (according to the ss09 scale) and 155 m for GISP2 (Meese/ Sowers scale), with typical strains of just a few per cent (Dahl-Jensen and others, 1993; Thorsteinsson, 1996). For the initial distribution of c axes at that depth, we take a fabric with slight anisotropy similar to that exhibited in the diagrams from GRIP and GISP2 ice cores (Thorsteinsson, 1996; Gow and others, 1997). All the rules of the algorithm depend on time and are applied at each step to the system of grains, except dynamic recrystallization. This last is built in the algorithm starting from the 4640th time-step (116 kyr BP), corresponding in GRIP to a temperature above $-15°C$ and a depth of approximately 2800 m, which is where coarse-grained ice was first observed (Thorsteinsson, 1996). This starting point for dynamic recrystallization also suits the estimations of Duval and Castelnau (1995) and the GISP2 data (Gow and others, 1997).

Figure 3 presents a comparison of the fabrics from the GRIP ice core with those obtained in the CA simulation, for four different ages. These fabrics represent four different regimes, dominated respectively by normal grain growth, polygonization, strong single-maximum anisotropy and dynamic recrystallization. It can be seen that the qualitative agreement is remarkable, and even a quantitative consonance is found, except for the last fabric (151 kyr BP). There are two main reasons for this last discrepancy. First, it has been
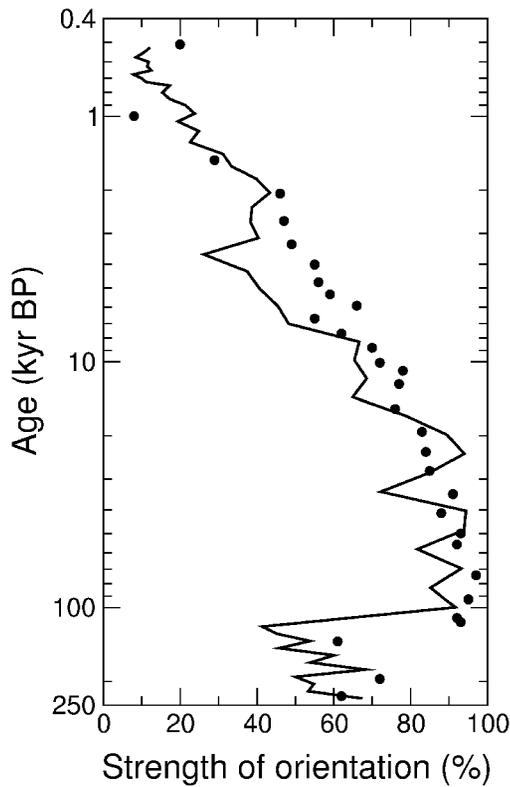
Fig. 4. Evolution of the strength of orientation R. Data from GRIP (circles) and CA simulation (solid line) are shown. Just for reference, R ≈ 40% corresponds to all c axes inclined at an angle of about π/4 from the vertical.

Fig. 5. Evolution of the mean grain-size D. Data from GRIP (circles) and CA simulation (solid line) are shown.

observed that the fine-grained ice from that particular age presents a high impurity content (especially calcium), which seems to inhibit the degradation of the single maximum by dynamic recrystallization (Thorsteinsson, 1996). Second, it is expected that shear stresses become significant at that depth even for the GRIP site (Hvidberg and others, 1997), reinforcing the maintenance of the single maximum.

Careful analysis of the last two fabrics also reveals some slight features of the simulation that deserve comment. The histogram of the third simulated fabric (54 kyr BP) indicates the formation of a weak circle girdle around the strong single maximum, which obviously cannot be accredited to dynamic recrystallization, since this is not activated by the program at that age. Such a structure seems to be formed by polygonization, and similar formations have often been observed in different simulations. Unlike girdles formed by dynamic recrystallization, such patterns tend to be feeble and sometimes transient, due to the action of kinematic rotation. On the other hand, it should be observed that, in the simulation, central peaks are hardly extinguished even under strong dynamic recrystallization, as evidenced in the last simulated fabric (151 kyr BP). This deficiency in the modelling is due to the assumption that the stress in each grain is equal to the applied bulk compression. Indeed, Equations (2) and (6) show that the dislocation density of crystals with vertical c axis cannot increase in this case. This impedes the polygonization and/or dynamic recrystallization of these grains, which can be consumed only through grain growth. By allowing the occurrence of intra- and intercrystal-line stresses, generated by the necessity of coherence within the aggregate, the dislocation density of vertically oriented grains would undergo a rapid increase, enabling them to poly-

gonize and/or recrystallize much more easily. In this case, the typical structure to be found in unconfined compression would be a small circle girdle, generated by polygonization and dynamic recrystallization processes, in agreement with laboratory and field observations (Budd, 1972; Budd and Jacka, 1989; Jacka and Li, 2000).
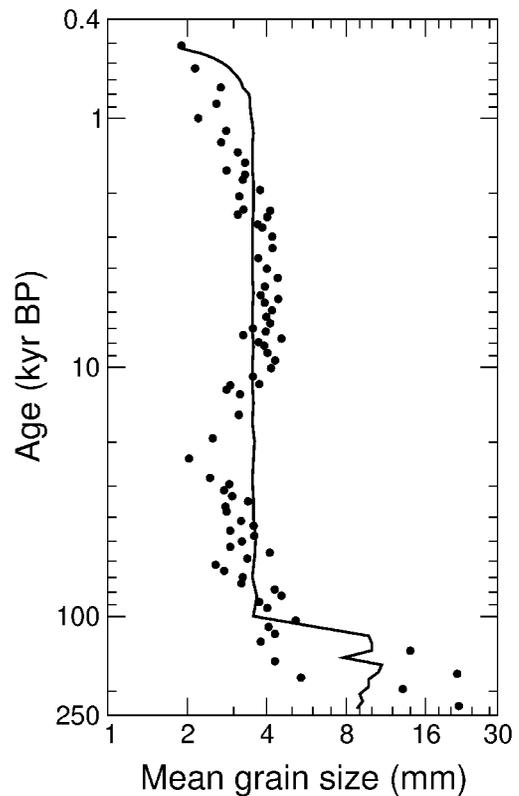
Finally, comparisons of the GRIP data with the simulated results for the evolution of the strength of fabric $R(t)$ and the mean grain-size $D(t)$ are given in Figures 4 and 5. The first quantity is defined by the formula (see, e.g., Castelnau and others, 1996; Thorsteinsson, 1996)

$$R\,(\%) = \left(2\frac{\|\sum_{k=1}^{M} \boldsymbol{n}_k \|}{M} - 1 \right) \times 100 , \qquad (8)$$

with $0\% \le R \le 100\%$ the two extrema corresponding to an isotropic distribution and a perfect alignment of c axes, respectively. It can be seen from Figure 4 that simulation and field data agree very well over the whole time interval, except for some casual numerical perturbations without physical significance (e.g. about 4 kyr BP). On the other hand, the correlation between observed and simulated mean grain-sizes in Figure 5 is qualitatively rough. The main reason for this is the fact that, in the model, the normal grain-growth rate K in Equation (4) is assumed to be a material constant, while in practice it should be a function, at least, of temperature and impurity content (Jacka and Li, 1994; Alley and Woods, 1996; Thorsteinsson and others, 1997; De La Chapelle and others, 1998). In fact, the hypothesis of a diagenetic-temperature memory influence on K cannot yet be ruled out (Petit and others, 1987). Moreover, detailed analyses of grain-boundary mobility in diverse materials have shown that the crystallographic misorientation across the boundary can have a strong influence on the grain-growth

549

kinetics (Heckelmann and others, 1992; Humphreys and Hatherly, 1996; Doherty and others, 1997). Finally, it must be remembered that Expression (5) for the misorientation subgrain angle is a gross approximation.

All these comments suggest that expressions much more complex than Equation (4) with $K =$ const. and Expression (5) are needed, in order to reproduce realistically the evolution of grain-size in polar ice cores. Such improved expressions should slow down grain-boundary migration and retard the onset of polygonization, tending to promote a time-dependent grain-growth rate as well as the marked reduction in mean grain-size observed in GRIP and GISP2 ice cores during the Last Glacial Maximum, about 21 kyr BP (Paterson, 1991; Gow and others 1997; Thorsteinsson and others, 1997).

CONCLUSION

We have proposed a model for simulations of texture and fabric development in polycrystalline ice based on a CA algorithm, developed by D. Ktitarev in collaboration with G. Gödert and K. Hutter, which allows us to consider simultaneously several microstructural mechanisms, from kinematic rotation to recrystallization processes. Due to the flexibility of the model in combining and updating rules for the evolving grain-size and crystallographic orientation distributions, a wide variety of physical hypotheses for ice-microstructure evolution are easily testable.

Although this preliminary attempt is presently constrained to a one-dimensional description of a hypothetical ice core, comparison of the simulation predictions with data from GRIP and GISP2 ice cores was satisfactory and provided valuable guidelines for the further development of more realistic models. Among the most significant improvements seen to be required are: the need for a two-dimensional generalization of the modelling, able to incorporate horizontal shear stresses and rotationally asymmetric fabrics; the allowance of stress fluctuations (i.e. intra- and intercrystalline stresses) within the aggregate, instead of the assumption of uniform stress; and the replacement of the simple rules adopted for grain growth and polygonization with more elaborate mechanisms depending, at least, on temperature and impurity content. These improvements have now been implemented, and their consequences will be presented elsewhere.

ACKNOWLEDGEMENTS

REFERENCES

Alley, R. B. 1988. Fabrics in polar ice sheets: development and prediction. *Science*, **240**(4851), 493–495.

Alley, R. B. 1992. Flow-law hypotheses for ice-sheet modelling. *J. Glaciol.*, **38**(129), 245–256.

Alley, R. B. and G. A. Woods. 1996. Impurity influence on normal grain growth in the GISP2 ice core, Greenland. *J. Glaciol.*, **42**(141), 255–260.

Asaro, R. J. 1983. Micromechanics of crystals and polycrystals. *Adv. Appl. Mech.*, **23**, 1–115.

Ashby, M. F. 1970. The deformation of plastically non-homogeneous materials. *Philos. Mag.*, **21**(8), 399–424.

Azuma, N. and A. Higashi. 1985. Formation processes of ice fabric patterns in ice sheets. *Ann. Glaciol.*, **6**, 130–134.

Budd, W. F. 1972. The development of crystal orientation fabrics in moving ice. *Z. Gletscherkunde Glazialgeol.*, **8**(1–2), 65–105.

Budd, W. F. and T. H. Jacka. 1989. A review of ice rheology for ice sheet modelling. *Cold Reg. Sci. Technol.*, **16**(2), 107–144.

Castelnau, O., Th. Thorsteinsson, J. Kipfstuhl, P. Duval and G. R. Canova. 1996. Modelling fabric development along the GRIP ice core, central Greenland. *Ann. Glaciol.*, **23**, 194–201.

Cuffey, K. M., Th. Thorsteinsson and E. D. Waddington. 2000. A renewed argument for crystal size control of ice sheet strain rates. *J. Geophys. Res.*, **105**(B12), 27,889–27,894.

Dahl-Jensen, D., S. J. Johnsen, C. U. Hammer, H. B. Clausen and J. Jouzel. 1993. Past accumulation rates derived from observed annual layers in the GRIP ice core from Summit, Central Greenland. *In* Peltier, W. R., *ed. Ice in the climate system.* Berlin, etc., Springer-Verlag, 517–532. (NATO ASI Series I12.)

De La Chapelle, S., O. Castelnau, V. Lipenkov and P. Duval. 1998. Dynamic recrystallization and texture development in ice as revealed by the study of deep ice cores in Antarctica and Greenland. *J. Geophys. Res.*, **103**(B3), 5091–5105.

Derby, B. 1992. Dynamic recrystallization: the steady state grain size. *Scripta Metall. Mater.*, **27**, 1581–1586.

Doherty, R. D and 9 others. 1997. Current issues in recrystallization: a review. *Mater. Sci. Engineer.*, *Ser. A*, **238**(2), 219–274.

Duval, P. and O. Castelnau. 1995. Dynamic recrystallization of ice in polar ice sheets. *J. Phys.* (Paris), **IV**(5), Colloq. C3, 197–205. (Supplément au 3.)

Faria, S. H. and K. Hutter. 2001. The challenge of polycrystalline ice dynamics. *In* Kim, S. and D. Jung, *eds. Advances in Thermal Engineering and Sciences for Cold Regions.* Seoul, Society of Air-Conditioning and Refrigerating Engineers of Korea (SAREK), 3–31.

Fujita, S., M. Nakawo and S. Mae. 1987. Orientation of the 700-m Mizuho core and its strain history. *Proc. NIPR Symp. Polar Meteorol. Glaciol.* 1, 122–131.

Gagliardini, O. and J. Meyssonnier. 1999. Plane flow of an ice sheet exhibiting strain-induced anisotropy. *In* Hutter, K., Y. Wang and H. Beer, *eds. Advances in cold-region thermal engineering and sciences: technological, environmental and climatological impact.* Berlin, etc., Springer-Verlag, 171–182. (Lecture Notes in Physics 533.)

Glen, J. W. 1975. The mechanics of ice. *CRREL Monogr.* IIC2b.

Gödert, G. and K. Hutter. 1998. Induced anisotropy in large ice sheets: theory and its homogenization. *Continuum Mech. Thermodyn.*, **10**(5), 293–318.

Gödert, G. and K. Hutter. 2000. Material update procedure for planar transient flow of ice with evolving anisotropy. *Ann. Glaciol.*, **30**, 107–113.

Goetz, R. L. and V. Seetharaman. 1998a. Modelling dynamic recrystallization using cellular automata. *Scripta Mater.*, **38**, 405–413.

Goetz, R. L. and V. Seetharaman. 1998b. Static recrystallization kinetics with homogeneous and heterogeneous nucleation using a cellular automata model. *Metall. Mater. Trans.*, **29A**, 2307–2321.

Gow, A. J. 1969. On the rates of growth of grains and crystals in south polar firn. *J. Glaciol.*, **8**(53), 241–252.

Gow, A. J. *and 6 others.* 1997. Physical and structural properties of the Greenland Ice Sheet Project 2 ice cores: a review. *J. Geophys. Res.*, **102**(C12), 26,559–26,575.

Greve, R., B. Mügge, D. Baral, O. Albrecht and A. Savvin. 1999. Nested high-resolution modelling of the Greenland Summit region. *In* Hutter, K., Y. Wang and H. Beer, *eds. Advances in cold-region thermal engineering and sciences: technological, environmental and climatological impact.* Berlin, etc., Springer-Verlag, 285–306. (Lecture Notes in Physics 533.)

Heckelmann, I., G. Abbruzzese and K. Lücke. 1992. The role of grain boundary energy in texture controlled grain growth. *In* Abbruzzese, G., *ed. Grain growth in polycrystalline materials.* Zürich, Trans Tech Publications, 391–398. (Materials science forum 94-96.)

Hesselbarth, H. W. and I. R. Göbel. 1991. Simulation of recrystallization by cellular automata. *Acta Metall. Mater.*, **39**(9), 2135–2143.

Hondoh, T., H. Iwamatsu and S. Mae. 1990. Dislocation mobility for non-basal glide in ice measured by *in situ* X-ray topography. *Philos. Mag. A*, **62**(1), 89–102.

Humphreys, F. J. and M. Hatherly. 1996. *Recrystallization and related annealing phenomena.* Oxford, etc., Pergamon Press.

Hutter, K. 1983. *Theoretical glaciology; material science of ice and the mechanics of glaciers and ice sheets.* Dordrecht, etc., D. Reidel Publishing Co.; Tokyo, Terra Scientific Publishing Co.

Hutter, K. and L. Vulliet. 1985. Gravity-driven slow creeping flow of a thermo-viscous body at elevated temperatures. *J. Thermal Stresses*, **8**(1), 99–138.

Hvidberg, C. S., D. Dahl-Jensen and E. D. Waddington. 1997. Ice flow between

the Greenland Ice Core Project and Greenland Ice Sheet Project 2 boreholes in central Greenland. *J. Geophys. Res.*, **102**(C12), 26,851–26,859.

Jacka, T. H. and Li Jun. 1994. The steady-state crystal size of deforming ice. *Ann. Glaciol.*, **20**, 13–18.

Jacka, T. H. and Li Jun. 2000. Flow rates and crystal orientation fabrics in compression of polycrystalline ice at low temperatures and stresses. *In* Hondoh, T., *ed. Physics of ice core records*. Sapporo, Hokkaido University Press, 83–102.

Kamb, B. 1972. Experimental recrystallization of ice under stress. *In* Heard, H. C., I. Y. Borg, N. L. Carter and C. B. Raleigh, *eds. Flow and fracture of rocks*. Washington, DC, American Geophysical Union, 211–241. (Geophysical Monograph 16.)

Lile, R. C. 1978. The effect of anisotropy on the creep of polycrystalline ice. *J. Glaciol.*, **21**(85), 475–483.

Lipenkov, V. Y., N. I. Barkov, P. Duval and P. Pimienta. 1989. Crystalline texture of the 2083 m ice core at Vostok Station, Antarctica. *J. Glaciol.*, **35**(121), 392–398.

Lliboutry, L. A.. 1993. Anisotropic, transversely isotropic nonlinear viscosity of rock ice and rheological parameters inferred from homogenization. *Int. J. Plasticity*, **9**(5), 619–632.

Marx, V., F. R. Reher and G. Gottstein. 1999. Simulation of primary recrystallization using a modified three-dimensional cellular automaton. *Acta Mater.*, **47**(4), 1219–1230.

McConnel, J. C. 1891. On the plasticity of an ice crystal. *Proc. Roy. Soc. London*, **49**(299), 323–343.

Meyssonnier, J. and A. Philip. 1996. A model for the tangent viscous behaviour of anisotropic polar ice. *Ann. Glaciol.*, **23**, 253–261.

Meyssonnier, J. and A. Philip. 2000. Comparison of finite-element and homogenization methods for modelling the viscoplastic behaviour of a S2-columnar-ice polycrystal. *Ann. Glaciol.*, **30**, 115–120.

Montagnat, M. and P. Duval. 2000. Rate controlling processes in the creep of polar ice: influence of grain boundary migration associated with recrystallization. *Earth Planet. Sci. Lett.*, **183**(1–2), 179–186.

Nordenskjöld, A. E. 1861. Beitrag zur Kenntniss der Krystallformen einiger Oxide. *Ann. Phys. Chem.*, **4**(24), 612–627. (Poggendorff's Ann. 114.)

Paterson, W. S. B. 1991. Why ice-age ice is sometimes "soft". *Cold Reg. Sci. Tech.*, **20**(1), 75–98.

Paterson, W. S. B. 1994. *The physics of glaciers. Third edition*. Oxford, etc., Elsevier.

Peczak, P., M. J. Luton. 1994. The effect of nucleation models on dynamic recrystallization II. Heterogeneous stored-energy distribution. *Philos. Mag. B*, **70**(4), 817–849.

Petit, J. R., P. Duval and C. Lorius 1987. Long-term climatic changes indicated by crystal growth in polar ice. *Nature*, **326**(6108), 62–64.

Reuss, A. 1929. Berechnung der Fliessgrenze von Mischkristallen auf Grund der Plastizitätsbedingung für Einkristalle. *Z. Angew. Math. Mech.*, **9**(1), 49–58.

Sachs, G. 1928. Zur Ableitung einer Fließbedingung. *Z. Vereins Deutscher Ing.*, **72**(8), 734–736.

Sandström, R. and R. Lagneborg. 1975. A model for hot working occurring by recrystallization. *Acta Metall.*, **23**(3), 387–398.

Steinemann, S. 1958. Experimentelle Untersuchungen zur Plastizität von Eis. *Beitr. Geol. Schweiz, Ser. Geotechnische — Hydrologie* 10.

Svendsen, B. and K. Hutter. 1996. A continuum approach for modelling induced anisotropy in glaciers and ice sheets. *Ann. Glaciol.*, **23**, 262–269.

Thorsteinsson, Th. 1996. Textures and fabrics in the GRIP ice core, in relation to climate history and ice deformation. *Ber. Polarforsch*. 205.

Thorsteinsson, Th., J. Kipfstuhl and H. Miller. 1997. Textures and fabrics in the GRIP ice core. *J. Geophys. Res.*, **102**(C12), 26,583–26,599.

Thorsteinsson, T., E. D. Waddington, K. C. Taylor, R. B. Alley and D. D. Blankenship. 1999. Strain-rate enhancement at Dye 3, Greenland. *J. Glaciol.*, **45**(150), 338–345.

Van der Veen, C. J. and I. M. Whillans. 1994. Development of fabric in ice. *Cold Reg. Sci. Technol.*, **22**(2), 171–195.

Weertman, J. 1983. Creep deformation of ice. *Annu. Rev. Earth Planet. Sci.*, **11**, 215–240.